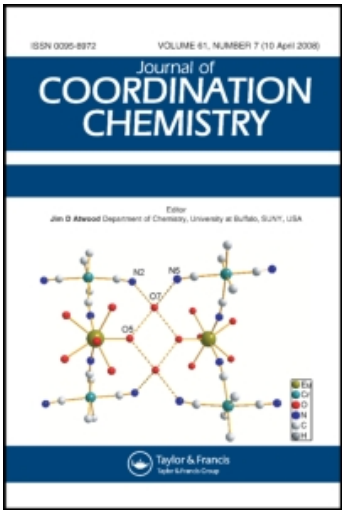

Journal of Coordination Chemistry
Publication details, including instructions for authors and subscription information:
http://www.informaworld.com/smpp/title~content=t713455674

Synthesis of new unsymmetrical "end-off" phenoxo bridged copper(II), nickel(II) and zinc(II) complexes: spectral, magnetic, electrochemical, catalytic, and antimicrobial studies

K. Shanmuga Bharathi[a]; S. Sreedaran[a]; P. Hema Priya[a]; A. Kalilur Rahiman[a]; K. Rajesh[a]; L. Jagadish[b]; V. Kaviyarasan[b]; V. Narayanan[a]
[a] Department of Inorganic Chemistry, School of Chemical Sciences, University of Madras, Chennai, India [b] Centre for Advanced Studies in Botany, University of Madras, Chennai, India

First published on: 29 July 2010

To cite this Article Shanmuga Bharathi, K. , Sreedaran, S. , Hema Priya, P. , Kalilur Rahiman, A. , Rajesh, K. , Jagadish, L. , Kaviyarasan, V. and Narayanan, V.(2009) 'Synthesis of new unsymmetrical "end-off" phenoxo bridged copper(II), nickel(II) and zinc(II) complexes: spectral, magnetic, electrochemical, catalytic, and antimicrobial studies', Journal of Coordination Chemistry, 62: 8, 1356 — 1372, First published on: 29 July 2010 (iFirst)
To link to this Article: DOI: 10.1080/00958970802570917
URL: http://dx.doi.org/10.1080/00958970802570917

Journal of Coordination Chemistry
Vol. 62, No. 8, 20 April 2009, 1356–1372

Taylor & Francis
Taylor & Francis Group

Synthesis of new unsymmetrical "end-off" phenoxo bridged copper(II), nickel(II) and zinc(II) complexes: spectral, magnetic, electrochemical, catalytic, and antimicrobial studies

K. SHANMUGA BHARATHI†, S. SREEDARAN†, P. HEMA PRIYA†, A. KALILUR RAHIMAN†, K. RAJESH†, L. JAGADISH‡, V. KAVIYARASAN‡ and V. NARAYANAN*†

†Department of Inorganic Chemistry, School of Chemical Sciences, University of Madras, Chennai, India
‡Centre for Advanced Studies in Botany, University of Madras, Chennai, India

(*Received 13 March 2008; in final form 21 July 2008*)

A new class of unsymmetrical end-off, aminomethylated *N*-methylpiperazine and aminomethylated diethanolamine binucleating ligands, 2-[*bis*(2-hydroxyethyl)aminomethyl]-6-[(4-methylpiperazin-1-yl)methyl]-4-methylphenol (HL^1) and 2-[*bis*(2-hydroxyethyl)amino-methyl]-6-[(4-methylpiperazin-1-yl)methyl]-4-acetylphenol (HL^2) were synthesized by following sequential aromatic Mannich reactions. Their mononuclear and binuclear Cu(II), Ni(II) and Zn(II) complexes have been synthesized and their formulation was confirmed by analytical and spectral analysis. The mononuclear Cu(II) complexes have a magnetic moment value close to the spin only value with four hyperfine EPR signals. The binuclear Cu(II) complexes have an antiferromagnetic interaction with a broad EPR signal. Electrochemical studies of the complexes reveal that all the redox processes are irreversible. Catecholase activity of Cu(II) complexes and the hydrolysis of 4-nitrophenylphosphate using Cu(II), Ni(II), and Zn(II) complexes were carried out. Spectral, magnetic, electrochemical, and catalytic behaviors of the complexes are compared on the basis of the *p*-substituent of the phenolic ring. Some of the complexes show significant growth inhibitory activity against pathogenic bacteria and fungi.

Keywords: Unsymmetrical "end-off" ligands; Magnetic properties; Electrochemistry; Catalytic activity; Antimicrobial activities; Mono and binuclear metal complexes

1. Introduction

The design and synthesis of cyclic or acyclic unsymmetrical binucleating ligands have been the subject of growing interest because the binuclear active sites of metalloenzymes are usually unsymmetrical with respect to the donor atoms as well as coordination numbers and/or the geometric arrangement [1–4]. For example, the unsymmetrical nature of the dicopper site in haemocyanin is demonstrated in the crystal structure of deoxyhaemocyanin and sequence homology studies on tyrosinases have shown that while one of the copper sites has been highly conserved throughout evolution, the

*Corresponding author. Email: vnnara@yahoo.co.in

ISSN 0095-8972 print/ISSN 1029-0389 online © 2009 Taylor & Francis
DOI: 10.1080/00958970802570917

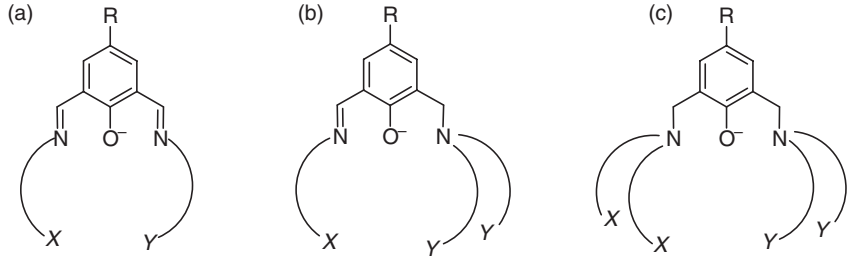

Scheme 1. Types of unsymmetrical "end-off" ligands.

structure of the second copper site has been quite variable. For most of the tyrosinases, three histidines are positioned to coordinate each of the copper ions, but for a few cases Cu_B is apparently only coordinated to two histidines, increasing interest in unsymmetrical binucleating ligands for modeling studies [1–5].

In phenol-based "end-off" complexes, in addition to the phenolate endogenous bridge the presence of one or two exogenous bridges made up of acetate, hydroxide, azide, cyanate, etc., give favorable distance between the bimetal centers resembling biosites [6, 7]. Diaminomethylated phenols have been used as templates for formation of dinuclear iron complexes which are active site mimics of enzymes like hemerythrine [8], methane monooxygenase [9] or ribonucleotide reductase [10]. The presence of diethanolamino arm enables the ligand to serve a variety of commercial applications such as corrosion inhibitors, surfactants, gas purification, and herbicides [11].

Complexes of symmetrical binucleating "end-off" compartmental ligands have been reported with a wide range of transition metal ions [12–14]. But due to the problems in synthesis, only limited unsymmetrical "end-off" complexes were reported. Three types of unsymmetrical "end-off" ligands are shown in scheme 1. Other than syntheses from Schiff-base condensation, reports are sparse [15, 16].

In continuation of our previous work [15], we have synthesized two new phenol-based unsymmetrical diaminomethylated "end-off" ligands 2-[*bis*(2-hydroxyethyl)aminomethyl]-6-[(4-methylpiperazin-1-yl)methyl]-4-methylphenol (HL^1) and 2-[*bis*(2-hydroxyethyl)aminomethyl]-6-[(4-methylpiperazin-1-yl)methyl]-4-acetylphenol (HL^2) by sequential aromatic Mannich reactions. The ligands have one amine tridentate chelating arm possessing NO_3 coordination site and one amine bidentate chelating arm possessing N_2O coordination attached to the 2- and 6-positions of the phenolic ring. They form mononuclear and homo binuclear copper(II), nickel(II), and zinc(II) complexes as "asymmetric donors" with respect to the two metal ions. The spectral, electrochemical, magnetic, and catalytic studies of these complexes are also discussed. Some of the complexes were screened for antibacterial and antifungal activities.

2. Experimental

2.1. *Analyses and physical measurements*

Elemental analyses were obtained using a Haereus C, H, N rapid analyzer. The atomic absorption spectral data were recorded using a Varian spectra AA-200 model atomic

absorption spectrophotometer. ^{1}H NMR spectra were recorded using a JEOL GSX 400 MHz NMR spectrometer. Mass spectra were obtained on JEOL DX-303 and JEOL SX-102 (FAB) mass spectrometers. IR spectra were recorded on a Shimadzu FT-IR 8300 series spectrophotometer with KBr disks from 4000 to 400 cm^{-1}. Electronic spectral studies were carried out on a Hitachi 320 spectrophotometer in the range of 200–1100 nm. X-band ESR spectra were recorded at 25°C on a Varian EPR-E 112 spectrometer using diphenylpicrylhydrazine (DPPH) as the reference. Room temperature magnetic moments were measured on a PAR vibrating sample magnetometer Model-155. Variable temperature magnetic moments were measured on an EG & G Princeton applied research VSM model 4500. Molar conductivity was measured by using an Elico digital conductivity bridge model CM-88 using freshly prepared solution of the complex in dimethylformamide. Cyclic voltammograms were obtained on a CHI-600A electrochemical analyzer. The measurements were carried out under oxygen-free condition using a three-electrode cell in which a glassy carbon electrode was the working electrode, a saturated Ag/AgCl electrode was the reference electrode and platinum wire was used as the auxiliary electrode. A ferrocene/ferrocenium (1+) couple was used as an internal standard; $E_{1/2}$ of the ferrocene/ferrocenium (Fc/Fc^+) couple under the experimental condition is 470 mV. Tetra(*n*-butyl)ammonium perchlorate (TBAP) was used as the supporting electrolyte. The catalytic oxidation of catechol to *o*-quinone by the copper complexes and the hydrolysis of 4-nitrophenylphosphate by the copper, nickel, and zinc complexes were studied at 10^{-3} M in dimethylformamide. The reaction was followed spectrophotometrically by choosing the strongest absorbance of *o*-quinone at 390 nm and monitoring the increase in the absorbance; hydrolysis of *p*-nitrophenylphosphate was monitored by following the UV absorbance change at 420 nm (assigned to the 4-nitrophenolate anion) as a function of time. A plot of $\log(A_\alpha/A_\alpha - A_t)$ *versus* time was made for each complex and the rate constants for the catalytic oxidation and the hydrolysis of 4-nitrophenylphosphate were calculated.

2.2. *Materials and safety note*

Formaldehyde solution, *N*-methylpiperazine, diethanolamine, *p*-cresol and *p*-hydroxyacetophenone were purchased from Qualigens and used as such. Methanol, acetonitrile and dimethylformamide were purchased from Qualigens and distilled before use. TBAP used as supporting electrolyte in electrochemical measurement was purchased from Fluka and recrystallized from hot methanol. (Caution! All perchlorate salts are explosive and hence care should be taken while handling.) All other chemicals and solvents were of analytical grade and used as received without purification. The metal salts were in the hydrated form, i.e. $Cu(OAc)_2 \cdot H_2O$, $Ni(OAc)_2 \cdot 4H_2O$, and $Zn(OAc)_2 \cdot 2H_2O$.

2.3. *Preparation of precursor compounds*

2.3.1. Preparation of 2-[(4-methylpiperazin-1-yl)methyl]-4-methylphenol (PC-1). A mixture of 4-methylphenol (5.23 mL, 0.05 mol), *N*-methylpiperazine (5.54 mL, 0.05 mol) and formaldehyde solution (37%) (3.77 mL, 0.05 mol) in methanol (50 mL) were treated at 50°C for 12 h. A 3 mL portion of formaldehyde was added after 6 h

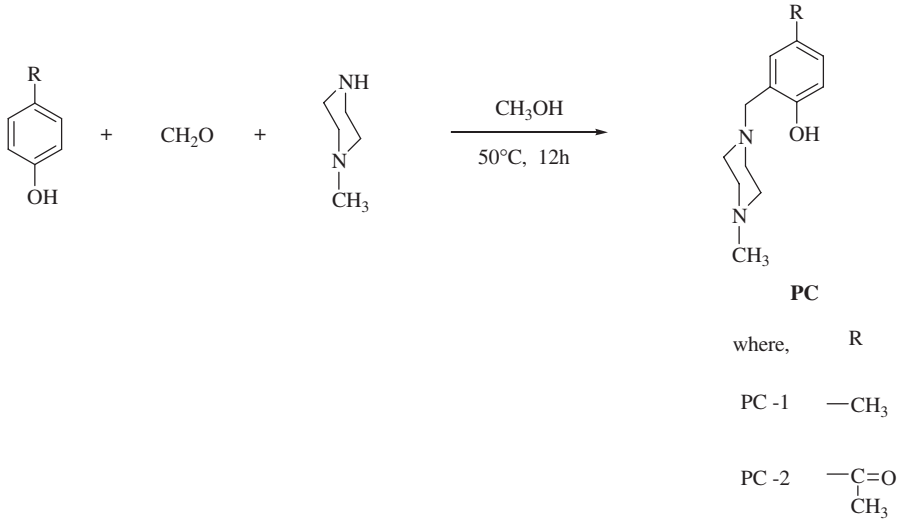

Scheme 2. Synthesis of precursor compounds.

(scheme 2) during the course of the reaction. Then, methanol was evaporated under vacuum and the resulting oil was extracted with chloroform. The crude compound was purified by column chromatography using chloroform : methanol mixture (98 : 2) as eluent to give a pale yellow oily compound. Yield: 5.61 g (51%), Mass (EI) *m/z*: 222.30. Anal. Calcd for $C_{13}H_{20}N_2O$: C, 70.87; H, 9.15; N, 12.72. Found: C, 70.96; H, 9.25; N, 12.65%. ^{1}H NMR (δ ppm in $CDCl_3$) ~2.23 (s, 3H), ~2.30 (s, 3H), ~2.53 (br s, 8H), ~3.65 (s, 2H), 6.70–6.94 (m, 3H).

2.3.2. Preparation of 2-[(4-methylpiperazin-1-yl)methyl]-4-acetylphenol (PC-2). The above similar procedure was used for preparation of precursor compound PC-2 by using 4-acetylphenol (6.81 g, 0.05 mol), instead of 4-methylphenol. In this case a pale brown compound was obtained. Yield: 6.95 g (56%). m.p.: 94°C. Mass (EI) *m/z*: 248.30. Anal. Calcd for $C_{14}H_{20}N_2O_2$: C, 67.72; H, 8.12; N, 11.28. Found: C, 67.78; H, 8.08; N, 11.37(%). ^{1}H NMR (δ ppm in $CDCl_3$): ~2.23 (s, 3H), ~2.44 (s, 3H), ~2.56 (br s, 8H), ~3.70 (s, 2H), 6.75–7.73 (m, 3H).

2.4. *Preparation of ligands*

2.4.1. Preparation of 2-[*bis*(2-hydroxyethyl)aminomethyl]-6-[(4-methylpiperazin-1-yl) methyl]-4-methylphenol (HL^1). Ligand-1 (HL^1) was synthesized by taking PC-1 (4.4 g, 0.02 mol) in methanol (100 mL) mixed with diethanolamine (1.92 mL, 0.02 mol) and formaldehyde solution (37%) (1.51 mL, 0.02 mol) and the solution was refluxed for 12 h. A 2 mL portion of formaldehyde was added at approximately 6 h. After that, methanol was evaporated under vacuum, the resulting oil was extracted with chloroform and the crude compound was purified by column chromatography using chloroform : methanol mixture (96 : 4) as eluent. A light brown oil was obtained (scheme 3). Yield: 4.32 g (64%). Mass (EI) *m/z*: 338.60. Anal. Calcd for $C_{18}H_{31}N_3O_3$: C,

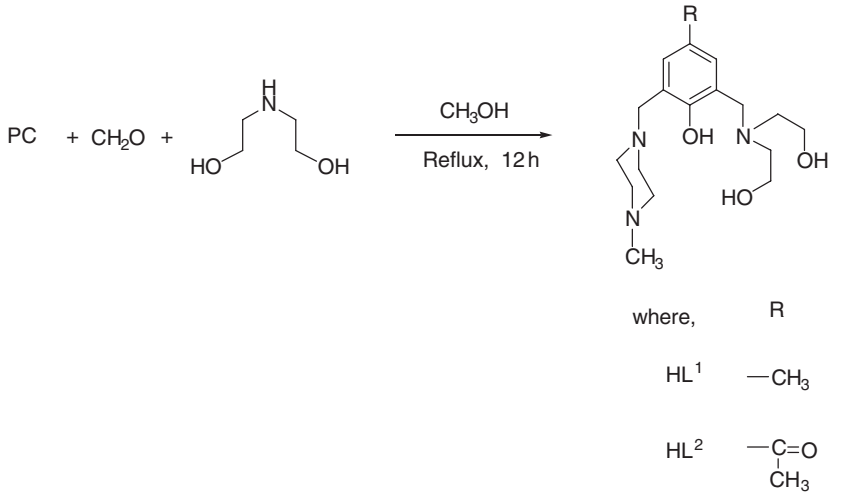

Scheme 3. Synthesis of unsymmetical "end-off" ligands.

64.07; H, 9.26; N, 12.45. Found: C, 64.19; H, 9.35; N, 12.37(%). Selected IR data (KBr disc, ν/cm^{-1}): 3200–3500, 1450. ^1H NMR (δ ppm in $CDCl_3$): ~2.16 (t, 2H), ~2.22 (s, 3H), ~2.30 (s, 3H), 2.50–2.60 (m, 12H), 3.55–3.82 (m, 8H), ~6.79 and 6.84 (s, 2H). UV–Vis[λ_{max}(nm) (ε, $M^{-1}\,cm^{-1}$)] in MeOH: 292 (21,100).

2.4.2. Preparation of 2-[*bis*(2-hydroxyethyl)aminomethyl]-6-[(4-methylpiperazin-1-yl)methyl] -4-acetylphenol (HL^2). The above similar procedure was used for the preparation of HL^2 by using PC-2 (4.97 g, 0.02 mol) instead of PC-1. The ligand HL^2 was obtained as a brown oily compound. Yield: 4.90 g (67%). Mass (EI) *m/z*: 365.80. Anal. Calcd for $C_{19}H_{31}N_3O_4$: C, 62.44; H, 8.55; N, 11.50. Found: C, 62.49; H, 8.53; N, 11.47. Selected IR data (KBr disc, ν/cm^{-1}): 3200–3500, 1670. ^1H NMR (δ ppm in $CDCl_3$): ~2.17 (t, 2H), ~2.23 (s, 3H), 2.46–2.54 (m, 15H), 3.59–3.78 (m, 8H), ~6.82 and 7.61 (s, 2H). UV–Vis[λ_{max}(nm) (ε, $M^{-1}\,cm^{-1}$)] in MeOH: 285 (21,900).

2.5. *Synthesis of mononuclear complexes*

2.5.1. Synthesis of mononuclear complexes of HL^1

2.5.1.1. *Synthesis of* $[CuL^1(OAc)]\cdot H_2O$. To a 40 mL methanol solution of HL^1 (1.01 g, 0.003 mol) was added $Cu(OAc)_2\cdot H_2O$ (0.60 g, 0.003 mol) dissolved in 20 mL of methanol and the solution was refluxed for 4 h. Then, the solution was filtered hot and allowed to stand at room temperature. After slow evaporation of the solvent at 25°C, a dark green compound was obtained and recrystallized from acetonitrile (scheme 4). Yield: 1.01 g (71%). Anal. Calcd for $[C_{20}H_{33}N_3O_5Cu]\cdot H_2O$: C, 50.35; H, 7.39; N, 8.81; Cu, 13.32. Found: C, 50.42; H, 7.33; N, 8.89; Cu, 13.41(%). Selected IR data (KBr disc, ν/cm^{-1}): 3200–3500, 1456. UV–Vis[λ_{max}(nm) (ε, $M^{-1}\,cm^{-1}$)] in MeOH: 605 (180), 365 (17,100), 291 (23,100). $g_{\|}$: 2.28, $g_{\perp}$: 2.07 and $A_{\|}$: 195. μ_{eff}: 1.71 BM.

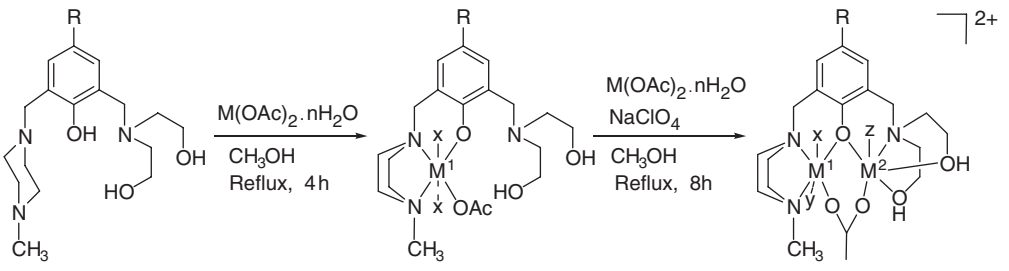

Where, R

HL^1 —CH_3

HL^2 —C(=O)—CH_3

Complexes	M	x
1,4	Cu	-
2,5	Ni	-
3,6	Zn	H_2O

Complexes	M^1	M^2	*x*	*y*	z
7,10	Cu	Cu	H_2O	-	-
8,11	Ni	Ni	H_2O	H_2O	H_2O
9,12	Zn	Zn	H_2O	H_2O	H_2O

Scheme 4. Synthesis of unsymmetical "end-off" complexes.

2.5.1.2. *Synthesis of* $[NiL^1(OAc)]\cdot H_2O$. The Ni(II) complex was prepared by following the above procedure using HL^1 (1.01 g, 0.003 mol) and $Ni(OAc)_2\cdot 4H_2O$ (0.75 g, 0.003 mol). A brown compound was obtained on recrystallization from acetonitrile. Yield: 0.95 g (67%). Anal. Calcd for $[C_{20}H_{33}N_3O_5Ni]\cdot H_2O$: C, 50.87; H, 7.47; N, 8.90; Ni, 12.43. Found: C, 50.96; H, 7.51; N, 8.85; Ni, 12.48(%). Selected IR data (KBr disc, ν/cm^{-1}): 3200–3500, 1453. UV–Vis[λ_{max}(nm) ($\varepsilon, M^{-1}\,cm^{-1}$)] in MeOH: 574 (144), 367 (17,600), 291 (23,400).

2.5.1.3. *Synthesis of* $[ZnL^1(OAc)]\cdot H_2O$. The Zn(II) complex was prepared by following the above procedure with $Zn(OAc)_2\cdot 2H_2O$ (0.66 g, 0.003 mol). A colorless compound was obtained on recrystallization from acetonitrile. Yield: 0.95 g (64%). Anal. Calcd for $[C_{20}H_{33}N_3O_5Zn(H_2O)_2]$: C, 48.34; H, 7.50; N, 8.46; Zn, 13.16. Found: C, 48.39; H, 7.43; N, 8.57; Zn, 13.24(%). Selected IR data (KBr disc, ν/cm^{-1}): 3200–3500, 1446. ^1H NMR (δ ppm in $CDCl_3$) ~2.00 (s, 3H), 2.16–2.77 (m, 24H), 3.61–3.89 (m, 8H), 6.85–7.27 (m, 2H). UV–Vis[λ_{max}(nm) ($\varepsilon, M^{-1}\,cm^{-1}$)] in MeOH: 292 (21,900).

2.5.2. Synthesis of mononuclear complexes of HL^2

2.5.2.1. *Synthesis of* $[CuL^2(OAc)]\cdot H_2O$. To a 40 mL methanol solution of HL^2 (1.10 g, 0.003 mol) was added $Cu(OAc)_2\cdot H_2O$ (0.60 g, 0.003 mol) dissolved in 20 mL of methanol and the solution was refluxed for 4 h. After the reaction completion, the solution was filtered hot and allowed to stand at room temperature. After slow evaporation of the solvent at 25°C, a dark green compound was obtained and recrystallized from acetonitrile (scheme 4). Yield: 0.98 g (65%). Anal. Calcd for $[C_{21}H_{33}N_3O_6Cu]\cdot H_2O$: C, 49.94; H, 6.98; N, 8.32; Cu, 12.58. Found: C, 49.89; H, 7.04; N, 8.39; Cu, 12.54(%). Selected IR data (KBr disc, ν/cm^{-1}): 3200–3500, 1678, 1452. UV–Vis[λ_{max}(nm) ($\varepsilon, M^{-1}\,cm^{-1}$)] in MeOH: 596 (160), 355 (15,900), 287 (23,600). $g_{\|}$: 2.21, $g_{\perp}$: 2.05 and $A_{\|}$: 186. μ_{eff}: 1.72 BM.

2.5.2.2. *Synthesis of* $[NiL^2(OAc)]\cdot H_2O$. The Ni(II) complex was prepared by the above procedure using HL^2 (1.10 g, 0.003 mol) and $Ni(OAc)_2\cdot 4H_2O$ (0.75 g, 0.003 mol). A brown compound was obtained on recrystallization from acetonitrile. Yield: 1.00 g (67%). Anal. Calcd for $[C_{21}H_{33}N_3O_6Ni]\cdot H_2O$: C, 50.42; H, 7.05; N, 8.40; Cu, 11.73. Found: C, 50.46; H, 7.12; N, 8.37; Cu, 11.71(%). Selected IR data (KBr disc, ν/cm^{-1}): 3200–3500, 1679, 1450. UV–Vis[λ_{max}(nm) ($\varepsilon, M^{-1}cm^{-1}$)] in MeOH: 570 (135), 360 (16,100), 289 (23,700).

2.5.2.3. *Synthesis of* $[ZnL^2(OAc)]\cdot H_2O$. The Zn(II) complex was prepared by the same procedure using HL^2 (1.10 g, 0.003 mol) and $Zn(OAc)_2\cdot 2H_2O$ (0.66 g, 0.003 mol). A colorless compound was obtained on recrystallization from acetonitrile. Yield: 0.96 g (61%). Anal. Calcd for $[C_{21}H_{33}N_3O_6Zn(H_2O)_2]$: C, 48.05; H, 7.10; N, 8.00; Zn, 12.46. Found: C, 48.12; H, 7.06; N, 8.05; Zn, 12.54(%). Selected IR data (KBr disc, ν/cm^{-1}): 3200–3500, 1680, 1449. UV–Vis[λ_{max}(nm) ($\varepsilon, M^{-1}cm^{-1}$)] in MeOH: 289 (22,500).

2.6. *Synthesis of binuclear complexes*

2.6.1. Synthesis of binuclear complexes of HL^1

2.6.1.1. *Synthesis of* $[Cu_2L^1(OAc)(H_2O)](ClO_4)_2$. A solution of HL^1 (0.67 g, 0.002 mol) in MeOH (40 mL) was added to $Cu(OAc)_2\cdot H_2O$ (0.80 g, 0.004 mol) in MeOH (20 mL) and refluxed for 11 h. The mixture was then reacted with two equivalents of $NaClO_4$ dissolved in 10 mL of methanol and further refluxed for 1 h. A dark green precipitate was collected on evaporation of the resulting solution to half the volume and allowing to standing at room temperature (25°C). A dark green compound was obtained on recrystallization from acetonitrile (scheme 4). Yield: 1.09 g (74%). Anal. Calcd for $[C_{20}H_{33}N_3O_5Cu_2(H_2O)](ClO_4)_2$: C, 32.48; H, 4.77; N, 5.68; Cu, 17.19. Found: C, 32.45; H, 4.84; N, 5.71; Cu, 17.25(%). FAB mass (m/z): 740.00. Selected IR data (KBr disc, ν/cm^{-1}): 3200–3500, 1605, 1455, 1102, 651. Conductance ($\Lambda_m/S\,cm^2\,mol^{-1}$) in DMF: 158. UV–Vis[$\lambda_{max}$(nm) ($\varepsilon, M^{-1}cm^{-1}$)] in MeOH: 672 (402), 369 (16, 700), 292 (23, 500). g: 2.10. μ_{eff}: 2.41 BM.

2.6.1.2. *Synthesis of* $[Ni_2L^1(OAc)(H_2O)_3](ClO_4)_2$. The Ni(II) complex was prepared by the above procedure using HL^1 (0.67 g, 0.002 mol) and $Ni(OAc)_2\cdot 4H_2O$ (1.00 g, 0.004 mol). A brown compound was obtained on recrystallization from acetonitrile. Yield: 1.07 g (70%). Anal. Calcd for $[C_{20}H_{33}N_3O_5Ni_2(H_2O)_3](ClO_4)_2$: C, 31.37; H, 5.13; N, 5.49; Ni, 15.33. Found: C, 31.42; H, 5.18; N, 5.47; Ni, 15.31(%). FAB mass (m/z): 766.00. Selected IR data (KBr disc, ν/cm^{-1}): 3200–3500, 1607, 1453, 1101, 650. Conductance ($\Lambda_m/S\,cm^2\,mol^{-1}$) in DMF: 162. UV–Vis[$\lambda_{max}$(nm) ($\varepsilon, M^{-1}cm^{-1}$)] in MeOH: 1037 (102), 800 (162), 632 (283), 377 (16,900), 287 (24,900).

2.6.1.3. *Synthesis of* $[Zn_2L^1(OAc)(H_2O)_3](ClO_4)_2$. The Zn(II) complex was prepared by the same procedure using HL^1 (0.67 g, 0.002 mol) and $Zn(OAc)_2\cdot 2H_2O$ (0.88 g, 0.004 mol). A colorless compound was obtained on recrystallization from acetonitrile. Yield: 1.06 g (68%). Anal. Calcd for $[C_{20}H_{33}N_3O_5Zn_2(H_2O)_3](ClO_4)_2$: C,

30.83; H, 5.04; N, 5.39; Zn, 16.78. Found: C, 30.89; H, 5.07; N, 5.32; Zn, 16.85(%). FAB mass (m/z): 780. Selected IR data (KBr disc, ν/cm^{-1}): 3460, 1610, 1456, 1100, 652. ^1H NMR (δ ppm in $CDCl_3$) ~2.01 (s, 3H), 2.16–2.77 (m, 26H), 3.64–3.94 (m, 8H), 6.88–7.30 (m, 2H). Conductance (Λ_m/S $cm^2\,mol^{-1}$) in DMF: 159. UV–Vis[λ_{max}(nm) (ε, $M^{-1}\,cm^{-1}$)] in MeOH: 292 (23, 600).

2.6.2. Synthesis of binuclear complexes of HL^2

2.6.2.1. *Synthesis of* $[Cu_2L^2(OAc)(H_2O)](ClO_4)_2$. A solution of HL^2 (0.73 g, 0.002 mol) in MeOH (40 mL) was added to $Cu(OAc)_2 \cdot H_2O$ (0.80 g, 0.004 mol) in MeOH (20 mL) and refluxed for 11 h. The mixture was then reacted with two equivalents of $NaClO_4$ dissolved in 10 mL of methanol and refluxed for another hour. A dark green precipitate was collected on evaporation of the resulting solution to half the volume and cooling by standing at room temperature (25°C). A dark green compound was obtained on recrystallization from acetonitrile (scheme 4). Yield: 1.12 g (73%). Anal. Calcd for $[C_{21}H_{33}N_3O_6Cu_2(H_2O)](ClO_4)_2$: C, 32.86; H, 4.60; N, 5.47; Cu, 16.56. Found: C, 32.91; H, 4.62; N, 5.41; Cu, 16.53(%). Selected IR data (KBr disc, ν/cm^{-1}): 3200–3500, 1680, 1610, 1460, 1100, 651. Conductance (Λ_m/S $cm^2\,mol^{-1}$) in DMF: 157. UV–Vis[λ_{max}(nm) (ε, $M^{-1}\,cm^{-1}$)] in MeOH: 668 (396), 362 (16, 100), 288 (24, 400). g: 2.11. μ_{eff}: 2.62 BM.

2.6.2.2. *Synthesis of* $[Ni_2L^2(OAc)(H_2O)_3](ClO_4)_2$. The Ni(II) complex was prepared by the same procedure using HL^2 (0.73 g, 0.002 mol) and $Ni(OAc)_2 \cdot 4H_2O$ (1.00 g, 0.004 mol). A brown compound was obtained on recrystallization from acetonitrile. Yield: 1.13 g (71%). Anal. Calcd for $[C_{21}H_{33}N_3O_6Ni_2(H_2O)_3](ClO_4)_2$: C, 31.77; H, 4.95; N, 5.29; Ni, 14.79. Found: C, 31.75; H, 5.01; N, 5.34; Ni, 14.78(%). Selected IR data (KBr disc, ν/cm^{-1}): 3455, 1678, 1602, 1461, 1102, 652. Conductance (Λ_m/S $cm^2\,mol^{-1}$) in DMF: 160. UV–Vis[λ_{max}(nm) (ε, $M^{-1}\,cm^{-1}$)] in MeOH: 1000 (110), 792 (135), 630 (278), 366 (16, 300), 286 (24, 600).

2.6.2.3. *Synthesis of* $[Zn_2L^2(OAc)(H_2O)_3](ClO_4)_2$. The Zn(II) complex was prepared by following the above procedure using HL^2 (0.73 g, 0.002 mol) and $Zn(OAc)_2 \cdot 2H_2O$ (0.88 g, 0.004 mol). A colorless compound was obtained on recrystallization from acetonitrile. Yield: 1.06 g (66%). Anal. Calcd for $[C_{21}H_{33}N_3O_6Zn_2(H_2O)_3](ClO_4)_2$: C, 31.25; H, 4.87; N, 5.20; Zn, 16.20. Found: C, 31.34; H, 4.93; N, 5.14; Zn, 16.23(%). Selected IR data (KBr disc, ν/cm^{-1}): 3450, 1681, 1603, 1447, 1103, 651. Conductance (Λ_m/S $cm^2\,mol^{-1}$) in DMF: 165. UV–Vis[λ_{max}(nm) (ε, $M^{-1}\,cm^{-1}$)] in MeOH: 290 (24, 100).

3. Results and discussion

New unsymmetrical end-off ligands having two different aminomethylated side arms have been synthesized by sequential aromatic Mannich reactions (schemes 2 and 3). The mononuclear and homo binuclear Cu(II), Ni(II), and Zn(II) complexes of the ligands were prepared as shown in scheme 4.

3.1. *Spectral studies*

3.1.1. Infrared spectra. The IR spectral data of the ligands show bands around 3350 and 3450 cm^{-1} due to phenolic and aliphatic OH [17] stretching frequencies, respectively. The sharp band at 1670 cm^{-1} for HL^2 shows the presence of aromatic carbonyl in the ligand and it remains unchanged in all the complexes, indicating that the carbonyl group is not coordinated. The broad band at 3450 cm^{-1} in all complexes is due to OH [17] and the presence of water. The peak at 1650 cm^{-1} in addition to the peak at 3450 cm^{-1} in all the binuclear complexes and zinc(II) mononuclear complexes shows that the water is coordinated to the metal [18]. The strong $\nu(CO_2)$ bands at 1450 cm^{-1} in mononuclear complexes indicates the presence of acetate. The binuclear complexes show the antisymmetric and symmetric $\nu(CO_2)$ vibrations of the acetate at 1600–1610 and 1445–1465 cm^{-1}, respectively. A $\Delta\nu$ value $[\Delta\nu = \nu_{as}(CO_2) - \nu_s(CO_2)]$ smaller than 200 cm^{-1} is typical of bridging carboxylate [19]. The presence of uncoordinated perchlorate in all the binuclear complexes is inferred from the single broad band around 1100 cm^{-1} (ν_3-antisymmetric stretching) not split and a band around 650 cm^{-1} (ν_4-antisymmetric bending). No band around 930 cm^{-1} (ν_2-symmetric stretching) due to coordinated perchlorate is observed, clearly indicating no coordinated perchlorate [20].

3.1.2. Electronic spectra. The electronic spectra of the mono and binuclear Cu(II) complexes and the mononuclear Ni(II) complexes exhibit three main transitions. A moderately intense peak in the range 280–300 nm is probably due to intra-ligand charge transfer transition [21]. A peak or shoulder at 350–370 nm is due to phenolato to copper(II) charge transfer [21]. Mononuclear Cu(II) complexes show λ_{max} at 600 nm due to *d–d* transition characteristic of square-planar geometry; binuclear Cu(II) complexes have the d–d transition at 670 nm indicative of "distorted square-pyramidal geometry" [22]. Mononuclear Ni(II) complexes show a single weak *d–d* band at 570 nm due to $^1A_{1g} \rightarrow {}^1A_{2g}$, indicating square-planar geometry [23]. The binuclear Ni(II) complexes show three *d–d* transitions at 1000 nm, 800 nm and 630 nm assigned to $^3A_{2g} \rightarrow {}^3T_{2g}$, $^3A_{2g} \rightarrow {}^3T_{1g}$, $^3A_{2g} \rightarrow {}^3T_{1g}$(P), characteristic of octahedral Ni^{2+} [24]. Mono and binuclear Zn(II) complexes display only ligand-centered charge transfer transitions in the UV region [23, 25].

The position of the phenolato-to-copper LMCT charge-transfer is sensitive to the electron density on copper [14, 16, 26]. There is a slight decrease in wavelength for the complexes when the electron-donating *p*-substituent, $-CH_3$ (365–377 nm) of the phenolic ring is replaced by electron-withdrawing $-C(O)CH_3$ (355–366 nm). In complexes of HL^2, the electron-withdrawing $-C(O)CH_3$ group at the para position delocalizes electron density, increasing the Lewis acidity of copper, thus shifting the phenolato-to-copper LMCT band to higher energy. For HL^1 complexes, the electron-donating $-CH_3$ increases electron density at the phenolic oxygen, causing the red shift [14, 16, 26].

3.1.3. ^{1}H-NMR spectra. The precursor compounds, ligands and their Zn(II) complexes were examined by ^{1}H-NMR spectra. In the precursor compounds singlets at 2.23 ppm in both cases are assigned to the *N*-methyl group, singlets at 2.30 and 2.44 ppm are assigned for Ar–CH_3 protons and $-C(O)CH_3$, respectively. The eight protons of the four methylene functions in the piperazine ring are a broad singlet at 2.53–2.56 ppm and singlets at 3.65–3.70 ppm are assigned to benzylic protons.

Multiplets in the range of 6.70–6.94 and 6.75–7.73 ppm are assigned to the three aromatic protons.

The two protons of the aliphatic –OH as a triplet at 2.16 and 2.17 ppm in the case of HL^1 and HL^2, respectively, and singlets at 2.22 and 2.23 ppm are assigned to three *N*-methyl protons. In HL^1, the singlet at 2.30 ppm is due to $Ar–CH_3$ and multiplets from 2.50–2.60 ppm are assigned to eight protons in the piperazine and four protons in the two $–O–CH_2$ functions. In HL^2, multiplets in the range 2.46–2.54 ppm are due to $–C(O)CH_3$, eight protons in the piperazine and four protons in the two $–N–CH_2–R$. Multiplets in the range 3.55–3.82 and 3.59–3.78 ppm are assigned to four protons in two benzylic functions and four protons in two $–O–CH_2$ functions in HL^1 and HL^2, respectively; singlets at 6.79, 6.84 and 6.82, 7.61 ppm are assigned to two aromatic protons.

In the ^{1}H-NMR spectra of the mononuclear Zn(II) complex of HL^1, multiplets in the range 2.16–2.77 ppm are assigned for 24 aliphatic protons which include four protons of two water molecules and excludes acetate which is a singlet at 2.00 ppm Benzylic protons, $–O–CH_2$ protons and aromatic protons are not changed much compared to the ligand. The ^{1}H-NMR spectra of the binuclear Zn(II) complex of HL^1 is similar to its mononuclear Zn(II) complex with the addition of one more water.

3.1.4. Mass spectral analysis. The EI mass spectra of the precursor compounds show the molecular ion peaks at $m/z = 222.30$ and 248.30, respectively. The molecular ion peaks (m/z) of HL^1 and HL^2 were at 338.60 and 365.80, respectively. The FAB mass spectra of binuclear Cu(II), Ni(II) and Zn(II) complexes of HL^1 show molecular ion peaks (M^+) at $m/z = 740$, 766 and 780, respectively. The spectra also show some peaks corresponding to various fragments of the complexes with many peaks due to isotopes. Thus, ^{1}H-NMR and mass spectral data confirm the structures of the precursor compounds, ligands and their complexes.

3.1.5. ESR spectra. The solid state ESR spectra of the copper(II) complexes were recorded in the X-band region at room temperature. ESR spectra of mononuclear **1** and **4** show four lines [27] with a nuclear hyperfine spin of 3/2, having g_{II} values 2.28 and 2.21, $g_\perp$ values of 2.07 and 2.05 and $A_\parallel$ 195 and 186 cm^{-1}. Broad spectra [27] without hyperfine splitting were obtained for dicopper complexes **7** and **10** with $g = 2.1$ centered at 3200 G, indicating the presence of an antiferromagnetic interaction between the two copper ions. From favorable orientation of the magnetic orbitals and in spite of the Cu–Cu separation, an antiferromagnetic interaction is observed.

3.2. *Magnetic studies*

The measured magnetic moment of **1** and **4** are 1.71 and 1.72 BM, very close to the spin only value (1.73 BM) expected for complexes having one copper(II) with a single unpaired electron in an essentially $dx^2–y^2$ orbital. Room temperature magnetic moment of **7** and **10** are 2.41 and 2.62 BM, respectively, showing interaction between copper centers. To find the magnetic exchange interaction, the magnetic moments of **7** and **10** were measured in the temperature range of 77–300 K, as shown in figure 1.

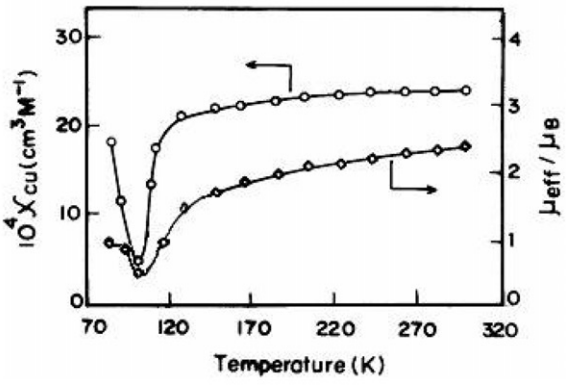

Figure 1. Temperature-dependence magnetic properties for $[Cu_2L^1(OAc)(H_2O)](ClO_4)_2$ (**7**).

The temperature dependence was interpreted using the modified Bleany–Bowers equation [28],

$$\chi_m = \{Ng^2\beta^2/3kT)[3 + \exp(-2J/kT)]^{-1}(1 - P) + (0.45P/T) + N_\alpha$$

in which the values of N_α, the temperature independent fraction and g are fixed as $120 \times 10^{-6}\,cm^3\,M^{-1}$ and 2.20, respectively. χ_m is the paramagnetic susceptibility per metal atom after correction for diamagnetism, P is the fraction of monomeric copper(II) impurities and $-2J$ is the singlet-triplet energy separation. The $-2J$ values were evaluated by a nonlinear regression analysis in which $-2J$, P and g are the variables. The values of the exchange integral $-2J$ for **7** and **10** are 43 and $26\,cm^{-1}$, indicative of weak antiferromagnetic coupling between copper(II) ions.

Complexes **7** and **10** show λ_{max} at 672 and 668 nm, respectively, indicating similar geometry. So the change in the magnetic exchange interaction difference is mainly influenced by the *p*-substituent of the phenolic ring. The electron-withdrawing group in the para position of the phenolic ring in **10** decreases the electron density on the copper centers [14, 16] and the antiferromagnetic coupling. Reduction in electron density weakens the Cu–O bond and reduces the spin exchange interaction [29]. The electron-donating CH_3 increases the electron density of the copper centers increasing antiferromagnetic coupling. The mononuclear Ni(II) complexes **2** and **5** are square planar and diamagnetic. The binuclear Ni(II) complexes **8** and **11** have magnetic moments of 3.03 and 3.05 BM, respectively, at room temperature, which is characteristic of Ni^{2+} in an octahedral site [24] and shows interaction between the two nickel centers. The variable temperature magnetic study of **8** and **11** from 77 to 300 K was interpreted using the modified Bleany-Bowers equation [28]. The values of the exchange integral $-2J$ for the binuclear Ni(II) complexes **8** and **11** are 52 and $39\,cm^{-1}$, respectively, indicative of weak antiferromagnetic coupling between the nickel(II) ions.

A significantly smaller $-2J$ value is observed for **10** than the copper(II) complex of 2,6-*bis*(4-methylpiperazin-1-yl-methyl)-4-acetylphenol [14]. There is a change of one aminomethylated diethanolamine side arm in the unsymmetrical ligand instead of one of two aminomethylated piperazinylmethyl side arms in the symmetrical ligand. The larger flexibility of the complex of the unsymmetrical ligand induces a larger

dihedral angle between the two copper containing planes and causes a smaller $-2J$ value [30].

3.3. *Electrochemical studies*

The conductance of all complexes was carried out in DMF. For mononuclear complexes, the conductance values were in the range 10–15 (Λ_m/S cm^2 mol^{-1}), indicating that the complexes are neutral. Conductance values of the binuclear complexes are in the range 150–170 (Λ_m/S cm^2 mol^{-1}), indicating that they are 1 : 2 electrolytes [31], showing no deprotonation of the two aliphatic OH protons during complexation [17].

3.3.1. Reduction at negative potential. Electrochemical properties of the complexes were studied by cyclic voltammetry in the potential range 0 to -1.8 V in DMF containing 0.1 M TBAP as supporting electrolyte and the data are summarized in table 1. The electronegativity and hard nature of phenoxide influence the electrochemical properties of the complexes [32, 33]. The ligands do not show reduction in the range studied (0 to -1.80 V *versus* Ag/AgCl) even in basic conditions (pH 7.5–9.5) (addition of NH_4OH); hence, the peaks obtained for the complexes are due to reduction of metal centers. Cyclic voltammograms for binuclear nickel(II) complexes are depicted in Supplementary Material. Cyclic voltammograms with different scan rates show no corresponding anodic peak in the cathodic direction, indicating irreversible process. The mononuclear copper(II), nickel(II) and zinc(II) complexes **1–6** show irreversible one-electron reduction in the cathodic region. The binuclear copper(II), nickel(II) and zinc(II) complexes **7–12** show two-step irreversible reductions. Controlled potential electrolysis was also carried out for the complexes at 100 Mv s^{-1} more negative to the cathodic peak, consuming one electron per molecule ($n = 0.95$), indicating that each wave corresponds to one electron process. The two reduction processes are assigned generically as follows,

$$M^{II}M^{II} \rightarrow M^{II}M^{I} \rightarrow M^{I}M^{I}$$

Table 1. Electrochemical data[a] for the complexes (reduction at cathodic potential).

No.	Complexes	E^1_{pc} (V)	E^2_{pc} (V)
1.	$[CuL^1(OAc)]\cdot H_2O$	−0.87	–
2.	$[NiL^1(OAc)]\cdot H_2O$	−0.96	–
3.	$[ZnL^1(OAc)(H_2O)_2]$	−0.97	–
4.	$[CuL^2(OAc)]\cdot H_2O$	−0.80	–
5.	$[NiL^2(OAc)]\cdot H_2O$	−0.89	–
6.	$[ZnL^2(OAc)(H_2O)_2]$	−0.91	–
7.	$[Cu_2L^1(OAc)(H_2O)](ClO_4)_2$	−0.85	−1.25
8.	$[Ni_2L^1(OAc)(H_2O)_3](ClO_4)_2$	−0.90	−1.39
9.	$[Zn_2L^1(OAc)(H_2O)_3](ClO_4)_2$	−0.92	−1.80
10.	$[Cu_2L^2(OAc)(H_2O)](ClO_4)_2$	−0.75	−1.16
11.	$[Ni_2L^2(OAc)(H_2O)_3](ClO_4)_2$	−0.78	−1.30
12.	$[Zn_2L^2(OAc)(H_2O)_3](ClO_4)_2$	−0.80	−1.60

Note: [a]Measured by CV at 50 mV/s. *E versus* Ag/AgCl conditions: GC working and Ag/AgCl reference electrodes; supporting electrolyte TBAP; concentration of complex: 1×10^{-3} M, concentration of TBAP: 1×10^{-1} M.

Copper, nickel and zinc, which are soft acids, favor coordination with nitrogen compared to oxygen. In complexation of these binucleating ligands, the first metal coordinates to the arm possessing N_2O coordination sites rather than NO_3; on reduction, the metal in NO_3 coordination will reduce first. This is also further supported by the higher flexibility of the diethanolamine arm possessing NO_3 coordination sites which hold the reduced cation easily and stabilizes the formation of Cu(I) [30]. This is shown from lowering the first reduction potential of the binuclear complexes when compared to that of the corresponding mononuclear complexes.

The reduction potential of the complexes is affected by the *p*-substituent of the phenyl ring, slightly higher for HL^1 than complexes of HL^2 [14, 16, 29].

3.3.2. Oxidation process at anodic potential. Mononuclear Ni(II) complexes **2** and **5** show an irreversible oxidation wave at +0.79 and +0.85V, respectively. The binuclear Ni(II) complexes **8** and **11** show two, one-electron processes at +0.85, +1.25 and +0.87, +1.36V, respectively (Supplementary Material). The irreversible two oxidation processes for the binuclear Ni(II) complexes are assigned generally as follows,

$$Ni^{II}Ni^{II} \rightarrow Ni^{III}Ni^{II} \rightarrow Ni^{III}Ni^{III}$$

3.4. *Kinetic studies*

3.4.1. Oxidation of pyrocatechol (catecholase activity). All the copper(II) complexes were subjected for catecholase activity as functional models for the metalloenzymes [34, 35]. The product *o*-quinone is stable and has a strong absorbance at 390 nm. Solutions of the complexes 10^{-3} mol dm^{-3} in dimethylformamide were treated with 100 equivalents of pyrocatechol in the presence of air. The course of the reaction was followed at 390 nm for 45 min at 5 min intervals. The slope was determined by the method of initial rates by monitoring the growth of the 390 nm band of the product *o*-quinone. A linear relationship for initial rate and complex concentration obtained for all the complexes shows first order dependence on the complex concentration. The plot of $\log(A_\alpha/A_\alpha - A_t)$ *versus* time for catecholase activity of **1** and **7** is shown in figure 2. The observed initial rate constant values are given in table 2. Under anaerobic conditions little product was formed, so the solvent was saturated with O_2 before the kinetic experiments. Oxygen participates directly in the catalytic cycle of the oxidation reaction, acting as a thermodynamic driving force for reoxidizing any copper(I) species generated in the cycle back to the active copper(II) species [13, 14, 27].

The structural features and electrochemical properties are important in determining the catalytic activity of the complexes. Changing from a mononuclear to a binuclear system, varying the *p*-substituents, varying the exogenous ligands and increasing the ring size lead to significant differences in the catalytic properties of the complexes. Binuclear copper(II) complexes show higher reactivity because oxidation of pyrocatechol to *o*-quinone requires two metal ions in close proximity [36]. Reactivity of the complexes differs significantly as the *p*-substituent of phenolic ring varies with HL^2 having enhanced catalytic activity, due to the electron-withdrawing *p*-substituent, $C(O)CH_3$ [16, 29]. If the reduction potential is too negative, the complex has decreased catalytic activity due to a more difficult reduction to copper(I), and a more positive

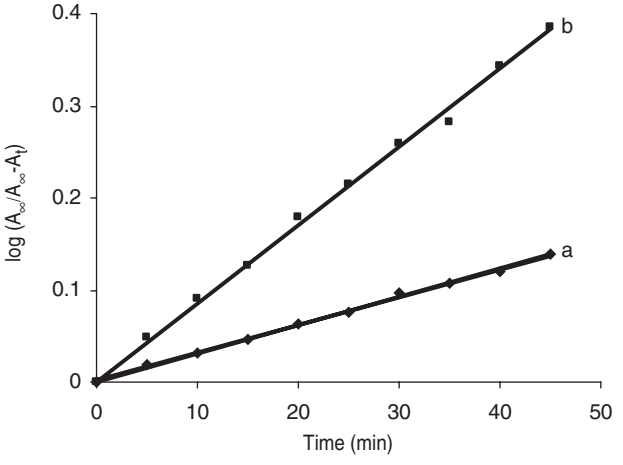

Figure 2. Catecholase activity of the copper(II) complexes: (a) $[CuL^1(OAc)]\cdot H_2O$ (**1**); (b) $[Cu_2L^1(OAc)(H_2O)](ClO_4)_2$ (**7**).

Table 2. Hydrolysis of 4-nitrophenylphosphate[a] and catecholase activity[a].

		Rate constant (k) ($\times 10^{-3}$) min^{-1}	
No.	Complexes	NPP	Catecholase
1.	$[CuL^1(OAc)]\cdot H_2O$	4.90	7.10
2.	$[NiL^1(OAc)]\cdot H_2O$	5.70	–
3.	$[ZnL^1(OAc)(H_2O)_2]$	4.80	–
4.	$[CuL^2(OAc)]\cdot H_2O$	5.30	7.80
5.	$[NiL^2(OAc)]\cdot H_2O$	6.70	–
6.	$[ZnL^2(OAc)(H_2O)_2]$	5.10	–
7.	$[Cu_2L^1(OAc)(H_2O)](ClO_4)_2$	14.40	19.60
8.	$[Ni_2L^1(OAc)(H_2O)_3](ClO_4)_2$	19.10	–
9.	$[Zn_2L^1(OAc)(H_2O)_3](ClO_4)_2$	13.60	–
10.	$[Cu_2L^2(OAc)(H_2O)](ClO_4)_2$	16.30	23.40
11.	$[Ni_2L^2(OAc)(H_2O)_3](ClO_4)_2$	23.50	–
12.	$[Zn_2L^2(OAc)(H_2O)_3](ClO_4)_2$	15.80	–

Notes: Concentration of the complexes: 1×10^{-3} M; Concentration of 4-nitrophenylphosphate: 1×10^{-1} M; Concentration of pyrocatechol: 1×10^{-1} M.
*Measured spectrophotometrically in DMF.

reduction potential of the complex gives a higher catalytic activity since the donor atoms stabilize copper(I).

3.4.2. Kinetic studies of hydrolysis of 4-nitrophenylphosphate. The hydrolytic activity of the mono and binuclear copper(II), nickel(II) and zinc(II) complexes towards 4-nitrophenylphosphate has been examined spectrophotometrically in DMF at 25°C in the presence of air. An absorption band typical of the *p*-nitrophenolate anion appeared at 420 nm and the intensity increased with time. No significant hydrolysis of the test substrate was observed when the metal complex was absent. Plots of $\log(A_\alpha/A_\alpha - A_t)$ *versus* time for hydrolysis of 4-nitrophenylphosphate activity of the complexes are shown in figure 3. A linear relationship for all the complexes shows a first-order dependence on the complex concentration for the systems. Initial rate constant values

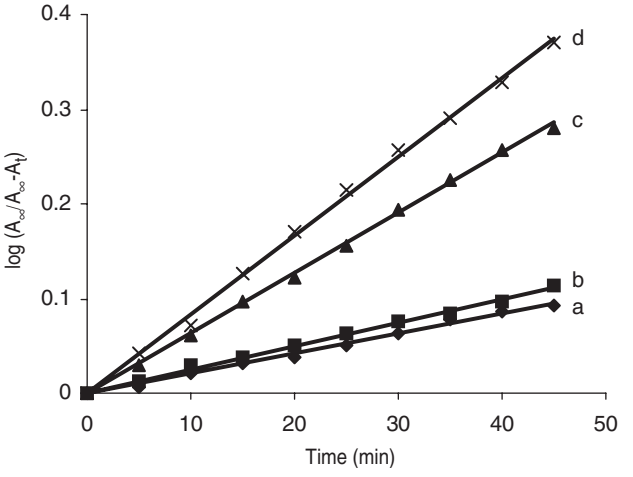

Figure 3. Hydrolysis of 4-nitrophenylphosphate by copper(II) and nickel(II) complexes: (a) $[CuL^1(OAc)]\cdot H_2O$ (**1**); (b) $[NiL^1(OAc)]\cdot H_2O$ (**2**); (c) $[Cu_2L^1(OAc)(H_2O)](ClO_4)_2$ (**7**); (d) $[Ni_2L^1(OAc)(H_2O)_3](ClO_4)_2$ (**8**).

for catalytic hydrolysis of 4-nitrophenylphosphate by the complexes are given in table 2. Binuclear complexes show higher reactivity than corresponding mononuclear complexes from two metal ions in close proximity. The mechanism of action has been explained with model complexes [37].

Hydrolysis of 4-nitrophenylphosphate by the Cu(II), Ni(II) and Zn(II) complexes shows the Ni(II) complexes have a higher rate constant than the Cu(II) and Zn(II) complexes, similar to earlier reports [13, 14]. Cu(II) complexes are more active towards oxidation of pyrocatechol than phosphate hydrolysis.

3.5. *Antimicrobial activity*

Complexes **1**, **2**, **7** and **8** were screened for antibacterial activity against *Staphylococcus aureus* (ATCC 6538p), *Bacillus cereus* (ATCC 11778), *Pseudomonas aeroginosa* (ATCC 9027), *Escherichia coli* (ATCC 25922) and *Klebsiella pneumoniae* (ATCC 29665), and antifungal activity against *Candida albicans* (ATCC 90028) by the cup plate method using Nutrient agar. Radial growth of the colony was recorded on completion of the incubation and the mean diameter for each complex was recorded at a concentration of $100\,\mu g\,ml^{-1}$. The average percentage inhibition of the bactericidal growth was compared using the Vincent [38] equation $I = 100(C - T)/C$, where $I =$ percentage inhibition, $T =$ average diameter of the bacterial growth on the tested plates and $C =$ average diameter of the growth on the control plates.

The screening data of the inhibition of the bacteria and fungi are given in table 3. Complex **7** showed activity against all bacteria except *E. coli*, highly active against the bacteria *B. cereus* and *K. pneumoniae* and moderately active against *S. aureus*, but only weakly active against *P. aeruginosa*. Complex **8** showed better activity against *P. aeruginosa* and was weakly active against *S. aureus*. Complex **1** showed only weak activity against the bacteria *S. aureus*, *B. cereus* and *K. pneumoniae*. Complexes **1**, **7** and **8** all show activity against *C. albicans*, with **7** showing better activity. All four complexes

Table 3. Screening data of complexes.

	Zone of inhibition (mm)					
	Antibacterial					Antifungal
Complexes	*S.a.*	*E.c.*	*B.c.*	*K.p.*	*P.a.*	*C.a.*
1.	12	–	13	14	–	12
2.	–	–	–	–	–	–
7.	21	–	27	31	19	22
8.	16	–	–	–	26	18

Notes: *Staphylococcus aureus* = *S.a.*; *Escherichia coli* = *E.c.*; *Bacillus cereus* = *B.c.*; *Klebsiella pneumonia* = *K.p.*; *Pseudomonas aeruginosa* = *P.a.*; *Candida albicans* = *C.a.* 0–10 mm = inactive; 10–20 mm = weakly active; 21–25 mm = moderately active; 26–35 mm = highly active. Concentration of the compound: 1 mg mL^{-1} in dimethylsulfoxide; quantity in each cup: 0.1 mL; Diameter of the cup: 10 mm; control of the antibacterial activity: norfloxacin; control of the antifungal activity: grisofulvin; and Solvent used: dimethylsulfoxide.

are inactive against *E. coli*. The mononuclear nickel(II) complex is inactive against all the bacteria and fungi.

4. Summary

Two new phenol-based unsymmetrical "end-off" ligands and their mono and binuclear Cu(II), Ni(II) and Zn(II) complexes have been prepared and characterized. Both the variable temperature magnetic and ESR spectral studies of the binuclear Cu(II) complexes show magnetic exchange between the two coppers. Electron-donating compared to electron-withdrawing *p*-substituent of the phenolic ring causes (a) a red shift in the LMCT-charge transfer band in electronic spectra and (b) an increase in antiferromagnetic interaction between copper(II) centers. Electron-withdrawing *p*-substituent causes anodic shift in the reduction potential of the metal.

Supplementary material

Magnetic and ESR spectral data for the binuclear Cu(II) and Ni(II) complexes and figures of cyclic voltammograms are given as supplementary material.

Acknowledgements

Financial support from University Grants Commission, New Delhi, India, is gratefully acknowledged. Recording of FAB mass spectra (CDRI Lucknow, India) is gratefully acknowledged.

References

[1] S.L. Roderick, B.W. Matthews. *Biochemistry*, **32**, 3907 (1993).
[2] M.A. Holmes, L. Le Trong, S. Turley, L.C. Sleker, R.E. Stenkamp. *J. Mol. Biol.*, **218**, 583 (1991).

[3] P. Nordlund, B.M. Sjoberg, H. Eklund. *Nature*, **345**, 593 (1990).
[4] S. Uozumi, M. Ohba, H. Okawa, D.E. Fenton. *Chem. Lett*., **26**, 673 (1997).
[5] S. Uozumi, H. Furutachi, M. Ohba, H. Okawa, D.E. Fenton, K. Shindo, S. Muruata, D.J. Kitko. *Inorg. Chem*., **37**, 6281 (1998).
[6] M. Suzuki, H. Furutachi, H. Okawa. *Coord. Chem. Rev*., **200**, 105 (2000).
[7] T.N. Sorrell, C. O'Connor, O.P. Anderson, J.H. Reibenspies. *J. Am. Chem. Soc*., **107**, 4199 (1985).
[8] A.S. Borovik, M.P. Hendrich, T.R. Holman, E. Munck, V. Papaefthymiou, L. Que Jr. *J. Am. Chem. Soc*., **112**, 6031 (1990).
[9] B.P. Murch, F.C. Bradley, L. Que Jr. *J. Am. Chem. Soc*., **108**, 5027 (1986).
[10] Y. Nishida, T. Akamatsu, M. Nasu. *Chem. Lett*., **20**, 1703 (1991).
[11] T. Esker, A. DeBoo, Y. Ishiwa. *Ethanolamines*, CEH Report (1999).
[12] H. Sakiyama, H. Tamaki, M. Kodera, N. Matsumoto, H. Okawa. *J. Chem. Soc., Dalton Trans*., 591 (1993).
[13] K. Shanmuga Bharathi, A. Kalilur Rahiman, K. Rajesh, S. Sreedaran, P.G. Aravindan, D. Velmurugan, V. Narayanan. *Polyhedron*, **25**, 2859 (2006).
[14] K. Shanmuga Bharathi, S. Sreedaran, A. Kalilur Rahiman, K. Rajesh, V. Narayanan. *Polyhedron*, **26**, 3993 (2007).
[15] (a) K. Shanmuga Bharathi, S. Sreedaran, A. Kalilur Rahiman, K. Rajesh, P. Anitha Aiswarya, V. Narayanan. *J. Coord. Chem*. (accepted for publication); (b) M. Lubben, B.L. Feringa. *J. Org. Chem*., **59**, 2227 (1994).
[16] (a) R. Mahalakshmy, R. Venkatesan, P. Sambasiva Rao, R. Kannappan, T.M. Rajendiran. *Transition Met. Chem*., **29**, 623 (2004); (b) T.M. Rajendiran, R. Kannappan, R. Mahalakshmy, J. Rajeswari, R. Venkatesan, P. Rao. *Trans. Met. Chem*., **28**, 447 (2003).
[17] M.J. Hossain, M. Yamasaki, M. Mikuriya, A. Kuribayashi, H. Sakiyama. *Inorg. Chem*., **41**, 4058 (2002).
[18] G.J. Kubas. *Organometallics*, **11**, 3396 (1992).
[19] G.B. Deacon, R.J. Phillips. *Coord. Chem. Rev*., **32**, 227 (1980).
[20] (a) K. Nakamoto. *Infrared and Raman Spectra of Inorganic and Coordination Compounds*, Wiley-Interscience, New York (1978); (b) M. Lachkar, R. Guilard, A. Atmani, A. DeCian, J. Fischer, R. Weiss. *Inorg. Chem*., **37**, 1575 (1998).
[21] J. Manonmani, M. Kandaswamy, V. Narayanan, R. Thirumurugan, S. Shanmuga Sundara Raj, G. Shanmugam, M.N. Ponnuswamy, H.K. Fun. *Polyhedron*, **20**, 3039 (2001).
[22] K. Bertoncello, G.D. Fallon, J.H. Hodgkin, K.S. Murray. *Inorg. Chem*., **27**, 4750 (1988).
[23] A.B.P. Lever. *Inorganic Electronic Spectroscopy*, 2nd Edn, Elsevier, Amsterdam (1984).
[24] T.C. Higgs, C.J. Carrano. *Inorg. Chem*., **36**, 298 (1997).
[25] F. Yilmaz, V.T. Yilmaz, S. Topcu, N. Menek. *J. Coord. Chem*., **56**, 903 (2003).
[26] E.W. Ainscough, A.G. Bingham, A.M. Brodie, J. Husbands, J.E.J. Plowman. *J. Chem. Soc., Dalton Trans*., 1701 (1981).
[27] M. Thirumavalavan, P. Akilan, M. Kandaswamy, K. Chinnakali, G. Senthilkumar, H.K. Fun. *Inorg. Chem*., **42**, 3308 (2003).
[28] B. Bleaney, K.D. Bowers. *Proc. R. Soc. Lond. Ser. A*, **214**, 451 (1952).
[29] M.J. Mac Lachlan, M.K. Park, L.K. Thompson. *Inorg. Chem*., **35**, 5492 (1996).
[30] A. Benzekri, P. Dubourdeaux, J.M. Latour, J. Laugier, P. Rey. *Inorg. Chem*., **27**, 3710 (1988).
[31] W.J. Geary. *Coord. Chem. Rev*., **7**, 81 (1971).
[32] K.D. Karlin, Y. Guitnech. *Inorg. Chem*., **35**, 219 (1987).
[33] F. Azevedo, C.T. Carrondo, B. Caseto, M. Convery, D. Domingues, C. Freire, T. Durate, K. Neilson, C. Santos. *Inorg. Chim. Acta*, **219**, 43 (1994).
[34] A. Neves, L.M. Rossi, A. Horn, I. Vencato, A.J. Bortoluzzi, C. Zucco, A.S. Mangrich. *Inorg. Chem. Commun*., **8**, 334 (1999).
[35] A. Neves, L.M. Rossi, I. Vencato, V. Drago, W. Hasse, R. Werner. *Inorg. Chim. Acta*, **281**, 111 (1998).
[36] A. Neves, L.M. Rossi, A.J. Bortoluzzi, B. Szpoganicz, C. Wiezbicki, E. Schwingel, W. Haase, S. Ostrovsky. *Inorg. Chem*., **41**, 1788 (2002).
[37] R.G. Clewley, H. Slebocka-Tilk, R.S. Brown. *Inorg. Chim. Acta*, **157**, 233 (1989).
[38] J.M. Vincent. *Nature*, **189**, 850 (1947).